

Research Article

Aminopropyl-Functionalized Silica CO₂ Adsorbents via Sonochemical Methods

Gregory P. Knowles^{1,2} and Alan L. Chaffee^{1,2}

¹Cooperative Research Centre for Greenhouse Gas Technologies, 17 Rainforest Walk, Monash University, Clayton, VIC 3800, Australia

²School of Chemistry, 17 Rainforest Walk, Monash University, Clayton, VIC 3800, Australia

Correspondence should be addressed to Gregory P. Knowles; greg.knowles@monash.edu and Alan L. Chaffee; alan.chaffee@monash.edu

Received 30 September 2015; Revised 28 January 2016; Accepted 2 February 2016

Academic Editor: Renal Backov

Copyright © 2016 G. P. Knowles and A. L. Chaffee. This is an open access article distributed under the Creative Commons Attribution License, which permits unrestricted use, distribution, and reproduction in any medium, provided the original work is properly cited.

Aminopropyl-functionalized hexagonal mesoporous silica (HMS) products, as are of interest for CO₂ capture applications, were separately prepared by mixing aminopropyltrimethoxysilane (APTS) and HMS in toluene via a conventional stirred reactor and via sonication assisted methods, to investigate the potential of sonication to facilitate the preparation of products with higher tether loadings and correspondingly higher CO₂ sorption capacities. Sonication was expected to improve both the dispersion of the substrate in the solvent and the diffusion of the silane throughout the mesoporous substrate. Structural properties of the products were determined by X-ray diffraction, N₂ adsorption/desorption (77 K), helium pycnometry, and elemental analysis, and CO₂ adsorption/desorption properties were determined via thermogravimetric and differential thermal analysis. The tether loadings of the sonication products (up to 1.8 tethers·nm⁻²) were found to increase with sonication time and in each case were greater than the corresponding product prepared by the conventional approach. It was also found that the concentration of the reagent mixture influenced the extent of functionalization, that the crude products cured effectively under N₂ flow as under vacuum, and that rinsing the crude products prior to curing was not essential. Sonication products with higher tether loadings were found to exhibit higher CO₂ sorption capacities as expected.

1. Introduction

Amidst a climate of record weather extremes, the global community is very concerned about the effects of a nonnatural global warming trend that is thought to be the result of ever increasing anthropogenic greenhouse gas emissions into the atmosphere [1–5]. The ever increasing CO₂ emissions resulting from air fired fossil fuel power generators are thought to be the main driver of this global warming trend [5]. Thus there is keen interest in strategies to reduce anthropogenic greenhouse gas emissions to halt/reverse this trend [6]. Capture/geosequestration of the CO₂ emissions from major point sources such as fossil fuel fired power stations is one such strategy [7, 8].

Aminopropyl-functionalized (-AP) hexagonal mesoporous silicas (HMS) were previously studied as potential sorbents for the capture of CO₂ from flue gas streams via

pressure swing adsorption as first reported by Delaney et al. in 2002 and Knowles et al. in 2004 [9]. Sayari also separately considered similar such materials for the postcombustion capture (PCC) of CO₂ around the same time using MCM-41 and SBA-15 and SBA-1 as silica supports [10]. Burwell Jr. & Leal had previously reported the use of aminopropyl-functionalized silica gels as CO₂ adsorbents [11].

Separation of CO₂ from the mixed gas streams was expected via the reversible formation of ammonium carbamate species, one CO₂ molecule adsorbed per two amine groups [12]. It was anticipated that the higher surface area of the HMS substrate coupled with the fact that the surface area is more uniformly distributed in mesoporous channels would lead to products with greater amine content per unit mass than conventional silica gel substrates and, in turn, to sorbents with greater CO₂ capacities. Indeed, the HMS substrate did lead to products with higher amine content per

unit mass (up to 1.5 tethers-nm⁻²) and higher CO₂ capacities as predicted [9]. The functionalized products were prepared by silylation of the silica substrates via conventional stirred reactor treatment with aminopropyltrimethoxysilane (APTS) in toluene, either at room temperature or in refluxing solvent [9].

The tether loadings achieved for the HMS substrates were found to decrease with decreasing pore diameter [9]. Prior to this, Walcarius et al. found that the tether densities achieved for a series of aminopropyl-gels were also decreased with decreasing substrate pore diameter [13]. As the channel diameter of a HMS substrate is reduced, it can be readily understood that each tethered aminopropyl group would occupy a greater fraction of the available substrate surface area due to the narrower porosity (greater angle of curvature) of the substrate. However the tether loadings achieved were significantly less than the levels which would correspond to stoichiometric modification of the substrate surface, based on estimated surface silanol contents. Thus, it was anticipated that higher tether loadings should be possible [9], a view subsequently supported by molecular modeling simulations [14].

A possible reason for the limit on the loadings achieved may be poor diffusion of the aminoalkylsilane modifier (trimethoxy-aminopropyl-silane) into the mesopores of the substrate [9]. Walcarius et al. had previously reported that aminopropyl groups had a strong affinity for the surface of silica gel, albeit in aqueous solution, due to H-bonding interaction with the surface silanol groups [13]. Chaffee notes that this strong affinity is also very evident in molecular dynamics simulations, in the absence of solvent [14].

Landau et al. reported that sonication facilitated improved fixation of a close packed monolayer of amorphous nanoparticles of Mo and Co oxides into MCM-41 mesopores, leading to materials with improved loading compared to conventional treatment methods [15]. Sonication was thought to improve the loading by promoting chemical interaction between the nanoparticles and the silica surface, by overcoming limitations due to premature pore blockage, by improving degassing and wetting of the substrate, and by improving dispersion of the active phase precursors [15]. It is thought that the main event in sonochemistry is the creation, growth, and collapse of gaseous solvent bubbles, which can lead to localized temperatures as high as 5000°C [16]. Hence, it was thought that sonication might promote silylation interaction between APTS and the silica surface, disrupt limiting amine/silanol interactions, improve diffusion of APTS throughout the HMS substrate mesopores, and overcome premature pore blockage limitations so as to provide aminopropyl-functionalized HMS products with higher tether loadings [17]. It was thought that sonication might also promote the breakdown of HMS agglomerates into more discrete primary particles, thereby making more silica surface available to the silane.

Other strategies to prepare such materials with higher and/or improved tether loadings have included the use of porous structures with larger pore volumes such as SBA-15 [10, 18–24], PE-MCM-41 [25, 26], and MCF [27] and the use of frameworks with 3-dimensional pore structures such as MCM-48 [28].

Further strategies include the addition or preadsorption of water to promote polycondensation of the alkoxysilanes [24, 25, 29], multiple treatments with aminoalkylsiloxanes towards the stepwise growth of polysiloxanes [29], the use of CO₂ and HCl preadsorption on amine functionalized silicas and preabsorption of CO₂ and HCl by aminoalkylsiloxane precursors to inhibit amine-silanol/silica interactions (in conjunction with sonication) [29], and the modification of mesoporous silicas via treatment with vapor phase aminoalkylsiloxanes [30–34] and via the cocondensation of aminopropyltrialkoxysilane as silica source and costructure directing agent in the direct preparation of aminopropyl-functionalized ordered mesoporous framework materials [35, 36]. The vapor phase strategy reduces the otherwise substantial solvent requirement, the direct cocondensation step avoids the additional postsynthesis modification step altogether, and both thereby provide a potentially cheaper and more environmentally friendly option.

Of these, the vapor phase silylation method is of particular relevant interest. Ek et al. reported the -AP functionalization of EP-10_x silica gel (as a stationary phase in various types of chromatography) via treatment with vapor phase aminopropylsiloxanes with up to 2.1 -AP molecules per nm² [30] and up to 3.0 -AP molecules per nm² in a high density aminopropylsiloxane network (horizontal polymerization) via multiple alternating treatments with vapor phase aminopropylsiloxanes and gaseous water [31]. The vapor phase silylation process was reported to facilitate the controlled preparation of even surface saturated layers of aminosilanes whereas typical solvent mediated silylation processes lead to the uncontrolled formation of irregular three-dimensional multilayers of aminosilanes on the silica surface [30]. Knowles et al. reported the preparation of aminopropyl-, ethylenediaminepropyl-functionalized (-ED) and diethylenetriaminepropyl-functionalized (-DT) HMS via treatment of the silica substrate with vapor phase aminoalkylsiloxanes as potential adsorbents for the PCC of CO₂ [33]. Here -AP, -ED, and -DT functionalized HMS products were prepared with 0.8, 0.6, and 0.6 tethers per nm², respectively, after a single treatment. Reprocessing of the -AP product after initial curing (hydrolysis of alkoxy groups) was found to improve its -AP loading up to 1.5 tethers per nm²; these materials were found to adsorb up to 4.8 wt% CO₂ (293 K). Sripathi et al. also recently reported that vapor phase aminopropylsilylation of mesoporous alumina led to a homogenous layer of grafted molecules whereas grafting from liquid phase is affected by pronounced oligomerization of the precursor molecules resulting in relatively nonhomogenous grafting and ultimately in pore blocking [34].

Most recently Chaikittisilp et al. reported the preparation hyperbranched polyamine-oxide hybrid materials via the polymerization of aziridine (polyethyleneimine) and azetidene (polypropyleneimine) initiated by the contact of monomer vapors with the surfaces of silica and alumina as adsorbents for CO₂ for application to reducing the levels of atmospheric CO₂ to address global warming [37]. Their results suggest that such hybrid materials can be prepared over a wide range of preparative conditions with organic

contents comparable to or even higher than those from the standard liquid-phase method [37].

It is noted that recent interest has been expressed in particular with the preparation of diethylenetriaminepropyl-functionalized [25, 26, 38] and polyethyleneimine-functionalized [39, 40] mesoporous materials (comprising predominantly secondary amines) for CO₂ capture given the higher amine contents and thereby CO₂ capacities of these materials. Such secondary amines however exhibit less stability to oxidative degradation than primary amines in conjunction with solid state mesoporous materials [27, 38] and so the study of CO₂ sorbents comprising predominantly primary amines such as -AP [27] and polyallylamine [41] functionalized materials is of particular interest.

In the present work hexagonal mesoporous silica (HMS) is functionalized by treatment with aminopropyltrimethoxysilane (APTS) in toluene via sonochemical methods: sonication time, dispersion concentration, and curing methods are varied. An amine functionalized silica product is also prepared via 24-hour treatment of HMS with APTS at room temperature for comparison. The materials prepared were characterized by X-ray diffraction, N₂ ads/des @ 77 K, helium pycnometry, and CHN microelemental analysis. The extent of aminopropyl-functionalization achieved is discussed in the context of prior work to assess the potential of the various treatment processes to prepare products with higher tether loadings. CO₂ adsorption/desorption studies were conducted at both 20°C and 75°C via combined thermogravimetric analysis and differential thermal analysis (TGA/DTA) to compare with prior work. Sorption studies at the higher temperature were conducted to investigate the potential of the sorbents under likely process conditions.

2. Experimental

2.1. Preparation of Materials. The hexagonal mesoporous silica substrate HX was prepared via the neutral templating technique [42] with a dodecylamine template as previously reported [9], and template removal was by ethanol extraction.

The aminopropyl-functionalized HX product prepared via a conventional stirred reactor method was prepared as follows. 1.5 mL APTS was added to ~0.5 g HX dispersed in 150 mL of anhydrous toluene, and the mixture was then magnetically stirred for 24 hours at room temperature under a CaCl₂ guard. The solid fraction was subsequently collected over a sintered funnel, washed with fresh solvent, dried under vacuum at 145°C for 24 hours, and then cooled to room temperature to prepare the off-white amine-functionalized product A24.

The aminopropyl-functionalized HMS products prepared via sonication methods were prepared as follows. 4.0 mL APTS was combined with ~0.5 g samples of HX in 50 mL anhydrous toluene (100 mL conical flask), and the flasks were then covered with a parafilm seal, lowered into a 55°C Unisonics FXP 12 MM sonicating water bath, and sonicated for an extended period of time. Typically the crude products were then collected over a Gooch crucible, rinsed twice with 50 mL aliquots of fresh toluene, and then dried under vacuum at 150°C for 24 h. Products S1, S2, S4, and

S7 were each prepared via 1, 2, 4, and 7 hours of sonication treatment, respectively. Products S2-25 and S2-12 were each prepared as per S2 but were only initially dispersed in 25 mL and 12 mL of toluene, respectively. Product S2-NR was prepared as per S2; however the crude product was not rinsed prior to drying under vacuum. Product S2-N2 was prepared as per S2, except that the crude product was cured under N₂ flow rather than under vacuum.

2.2. Characterization of Materials. Powder X-ray diffraction (XRD) was conducted on a Scintag X-ray Diffractometer. Diffraction of CuK α radiation (1.54059 Å) was studied over the range 1–10 (2θ) at increments of 0.05 (2θ). An exponential decay function was applied to the raw diffraction data as an appropriate baseline signal correction, assuming Gaussian curve shape for the sample diffraction peaks. The distance between $d_{(100)}$ symmetry planes (d) was calculated from the peak diffraction angle using Bragg's Law. The separation of pore centres (PS) was calculated from the peak diffraction peak such that $PS = 2d/3^{0.5}$.

N₂ adsorption/desorption (a/d) @ 77 K was conducted on a Coulter Omnisorp 360CX gas sorption analyzer. BET surface areas were determined from the adsorption isotherm data collected over the partial pressure range 0.05–0.14 (~4 points). Mesopore volumes were estimated as the volume adsorbed at partial pressure 0.90. BJH pore size distributions were determined from the desorption isotherms.

Helium pycnometry was conducted on a Micromeritics Accupyc 1330 pycnometer. The products were dried under N₂ flow at ~105°C and then cooled to room temperature in a dessicator prior to analysis.

CHN elemental analysis was conducted by the Campbell Microanalytical Laboratory, Department of Chemistry, University Of Otago, Dunedin, New Zealand. The products were dried to constant mass under vacuum at 150°C prior to analysis.

The tether loading (TL), the amount of tethers in the products per unit substrate surface area, was calculated from the N content of the products (N_p), the surface area of the substrate materials (SA_s), and the mass of substrate per mass of the products (M_s/M_p) as shown by (1). M_s/M_p was calculated from the mass of the tether added to the substrate per mass of the product (M_T), assuming bidentate coordination of the silane to the substrate surface and hydrolysis of the residual alkoxy groups, and from M_H , the mass of substrate H per product mass that was lost to bind the tether to the substrate surface, as per (2) [38]. The calculations are

$$\begin{aligned} \text{TL (tethers} \cdot \text{nm}^{-2}) &= \frac{N_p \text{ (mol} \cdot \text{g}^{-1})}{M_s/M_p \text{ (g} \cdot \text{g}^{-1}) * SA_s \text{ (m}^2 \cdot \text{g}^{-1})} \\ &= \frac{6.022 * 10^{23} \text{ (tethers} \cdot \text{mol}^{-1})}{10^{18} \text{ (nm}^2 \cdot \text{m}^{-2})}, \end{aligned} \quad (1)$$

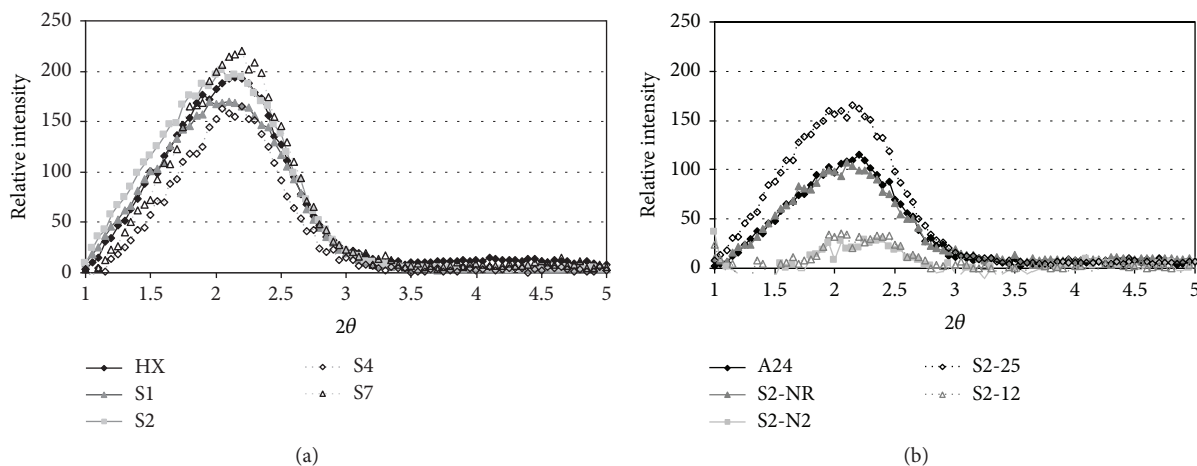


FIGURE 1: XRD patterns obtained for (a) HX, S1, S2, S4, and S7 and (b) A24, S2-NR, S2-N2, S2-25, and S2-12.

$$\frac{M_S}{M_P} (\text{g} \cdot \text{g}^{-1}) \quad (2)$$

$$= 1 (\text{g} \cdot \text{g}^{-1}) - M_T (\text{g} \cdot \text{g}^{-1}) + M_H (\text{g} \cdot \text{g}^{-1}).$$

CO₂ sorption experiments were conducted on a Setaram TAG24 Simultaneous Symmetrical Thermoanalyser. Samples were first dried to constant mass under dry Ar flow at 150°C then weighed into the instrument. The samples were redried to constant mass at 150°C and then cooled to the specified temperature, all under Ar flow. CO₂ partial pressure swing sorption studies were conducted at both 20°C and 75°C. Here the gas supply was first set to 90% CO₂ in Ar for 20 minutes to facilitate CO₂ adsorption; the gas supply was then returned to 100% Ar to facilitate desorption; the gas flow was maintained at a constant 70 mL per minute throughout the entire process. The samples were subsequently redried under Ar at 150°C, cooled to room temperature, and then reweighed on an external balance to verify sample mass integrity. The procedure was repeated with an empty cup to facilitate background correction of the sample data. CO₂ adsorption capacities were determined from the sample mass increase observed by the end of the 20-minute adsorption cycle. The heat of adsorption of CO₂ [$H_{\text{ads}}(\text{CO}_2)$] was determined from the combined TGA/DTA records obtained over the first ten minutes of the adsorption cycle.

3. Results/Discussion

3.1. Basic Characterisation of Materials. It is first noted that in all cases the APTS/HMS dispersions prepared via the sonication method were less opaque than the dispersions prepared via the conventional technique; hence sonication appeared to improve dispersion of the HMS substrate.

Figure 1 shows the XRD patterns obtained for each of the materials prepared. The diffraction pattern obtained for the substrate material, HX, exhibits a major peak centered at ~ 2.1 2θ and a second much weaker peak centered at ~ 4.4 2θ consistent with the preparation of a well ordered HMS type framework structure [42].

The diffraction patterns obtained for the functionalized products S1, S2, S4, S7, S2-NR, and S2-25 also exhibit a diffraction peak centered at ~ 2.1 2θ ; however the intensity of these peaks is in general less than that observed for the substrate material. These results suggest that all the products retained the ordered framework structure of the substrate; the weaker intensity of these peaks is thought to be due to the disordered presence of the tethers.

The patterns obtained for the functionalized products S2-N2 and S2-12 also exhibit diffraction at ~ 2.1 2θ angle, albeit with much less intensity, consistent with retention of the substrate framework structure. The particularly weak intensity for these samples may be due to the particular conditions (higher concentration of modifier) leading to a less ordered distribution of tethers within the pores, or possibly due to the formation of small agglomerations of polymerized aminopropylsiloxanes within the mesopores.

Figure 2 shows the N₂ adsorption/desorption isotherms obtained for each of the products. The isotherms obtained for the substrate HX exhibit a type 4 pattern and narrow hysteresis as expected for HMS [42]. The isotherms obtained for the functionalized products exhibit the same type 4 pattern and narrow hysteresis, but with reduced mesopore volume and narrower mesoporosity. Figure 2 also shows the BJH pore size distributions calculated for each material. These clearly show that, for each case, modification of HX led to a reduction in porosity consistent with functionalization of the substrate inside the mesopores.

Table 1 lists the surface areas (SA), pore volumes (PV), peak BJH pore diameters (PD), helium densities (HD), pore separations (PS), and the CHN compositions determined for each material. These results show that in each case modification of HX lead to a decrease in SA, PV, PD, and HD and an increase in C, H, and N content but did not significantly affect the PS. This is consistent with surface functionalization (aminoalkylsilylation) of the substrate and retention of the substrate framework structure. Furthermore these results show that the reductions in SA, PV, and PD and the increases in C, H, and N content were greater for the

TABLE I: Basic characterisation data.

	SA (m ² ·g ⁻¹)	C _{BET}	PV (mL·g ⁻¹)	PD (Å)	PS (Å)	HD (g·mL ⁻¹)	C (wt%)	H (wt%)	N (wt%)
^a ±error	5	4	0.01	<0.1	—	^b <0.01	<0.1	<0.1	<0.1
HX	849	77	0.80	28.9	52	2.04	3.2	1.5	0
A24	713	48	0.55	25.2	52	1.90	8.8	2.2	2.3
S1	712	55	0.56	24.4	52	1.96	8.0	2.1	2.6
S2	680	50	0.53	24.4	52	1.94	8.6	2.2	2.7
S4	712	44	0.53	24.3	51	1.98	8.7	2.3	2.7
S7	667	40	0.47	23.2	51	1.98	10.1	2.4	2.9
S2-NR	695	46	0.52	24.2	52	1.95	8.7	2.2	2.7
S2-N ₂	695	50	0.51	23.9	49	1.93	9.3	2.3	2.7
S2-25	667	46	0.48	23.5	52	1.93	9.3	2.3	2.9
S2-12	690	47	0.51	24.5	50	1.96	9.1	2.3	2.7

SA: BET surface area; C_{BET}: BET C constant; PV: pore volume; PD: BJH pore diameter; PS: separation of pore centres; HD: helium density.

^aError estimated from the average of the standard deviations obtained for duplicate measurements obtained for selected materials.

^bError listed was obtained from replicate analysis of a similar set of materials.

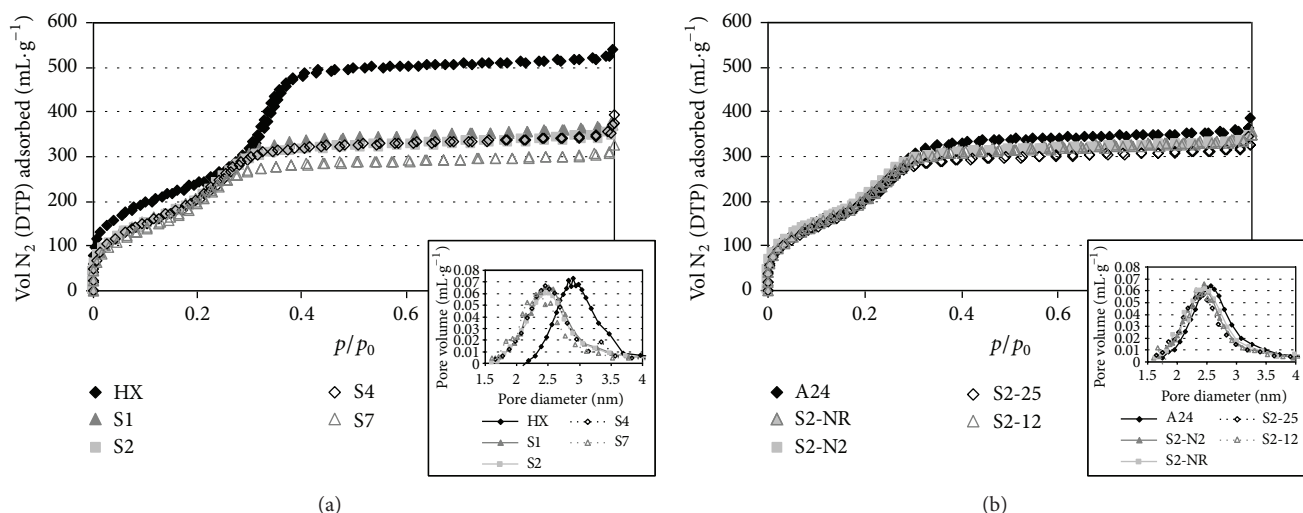


FIGURE 2: N₂ a/d 77 K isotherms with inset BJH pore size distributions obtained for (a) HX, S1, S2, S4, and S7 and (b) A24, S2-NR, S2-N2, S2-25, and S2-12.

materials prepared via the sonication methods. It is also noted that HX has a small but significant C and H content. This is attributed to incomplete template extraction, incomplete removal of the template extraction solvent, and/or (possibly) incorporation of the tetraethylorthosilicate precursor alkoxy groups into the framework structure.

Figure 3 shows the C/N molar ratios obtained for each of the products together with those predicted for monodentate, bidentate, and tridentate coordination of the silane to the substrate. Each of the products is thus found to have C/N ratios between the values expected for monodentate and tridentate coordination of the silane and, so, is consistent with aminopropyl-functionalization of the substrate. All the sonication products were found to have C/N ratios between that expected for bidentate and tridentate coordination of the silane. Since tridentate coordination of siloxanes is typically not favored [43, 44] and considered unlikely given steric difficulty [9], our interpretation is that, in each case, the silane was predominantly configured with bidentate coordination.

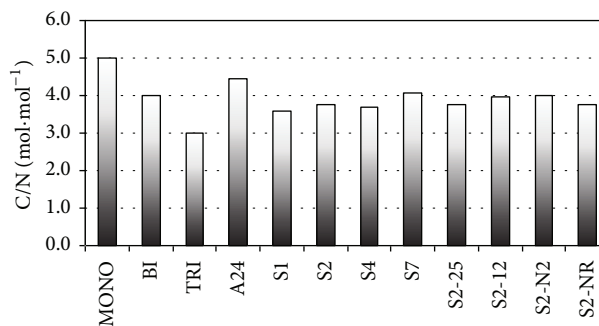


FIGURE 3: Ratio of C/N elemental composition of aminopropyl-functionalized products.

Product A-24, however, exhibited a significantly larger C/N ratio. This is thought to be due to the retention of residual C (from the template) in the HX that was used for its preparation. Thus, it is surmised that sonication facilitated

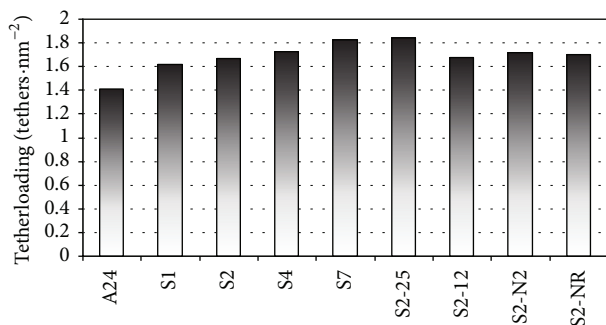


FIGURE 4: Tether loading calculated for of aminopropyl-functionalized products.

removal of most of this residual template, making more of the substrate surface available for modification leading, in turn, to higher tether loadings. It is noted that A24 has a lower HD than any of the sonication products, consistent with this interpretation.

Figure 4 shows the tether loading calculated for each of the product materials. The tether loading for product A24 was 1.4 tethers·nm⁻² of substrate surface, nearly identical to that reported previously for a sample prepared from a similar porosity HMS substrate (sample H5a-p2 in [9]).

3.1.1. Effect of Sonication. Figure 4 also shows that all the products prepared by the sonication method provided higher tether loadings than the conventionally prepared sample (A24). They are also improved upon the best cases (1.5 tethers·nm⁻²) for our previously reported aminopropyl-functionalised HMS products [9], as were prepared with similarly high APTS concentrations and APTS: silica surface area ratios. These results substantiate the hypothesis that sonication would improve on the loading otherwise achieved by the conventional stirred reactor as was understood. It probably does so by overcoming diffusion limitations and promoting chemical interaction between the silane alkoxy groups and the silica surface silanol groups. This is in accord with reports by Landau et al. [15] and Gedanken [16] and, by the same token, by constantly disrupting amine-silanol interactions.

3.1.2. Effect of Sonication Time. Figure 4 shows that the tether loading increased with sonication time. The best value of 1.8 tethers·nm⁻² was obtained for product S7 (7-hour sonication time). This is slightly less than the 2.1 tethers·nm⁻² reported achieved via the single step vapor phase silylation method [30]; however this may relate to the use of the larger pore volume lower surface area EP-10_x silica gel substrate in this case. The loading is however actually higher than the 0.9 aminopropyl- tethers·nm⁻² separately reported for the vapor phase silylation of a similar HMS product [33], though this may be due to differences in vapor phase treatment methods used. It is noted that longer treatment times and the use of higher intensity sonication might lead to higher loadings still, but these were not studied.

3.1.3. Effect of Dispersion Concentration. Figure 4 also shows that products S2-25 and S2-12 also achieved relatively high tether loadings of 1.8 and 1.7 tethers per nm², respectively, essentially the same as for S7 and S2, respectively. It is therefore concluded that increasing the dispersion concentration up to 0.02 g·mL⁻¹ can lead to a significant increase in tether loading; however a further increase in concentration did not. It may be that at concentrations higher than 0.04 g·mL⁻¹ polymeric siloxane agglomeration occurs, thereby limiting access to the substrate surface.

3.1.4. Effect of Postsonication Cleanup. In addition Figure 4 shows that S2-NR and S2-N2 have essentially the same tether loadings as S2 (1.7 tethers·nm⁻²). Hence it is concluded that the rinsing step is not essential and furthermore that the products are cured just as effectively under N₂ flow as they are under vacuum.

3.2. CO₂ Adsorption/Desorption

3.2.1. CO₂ Adsorption/Desorption at 20°C. Figure 5 shows the typical gravimetric records obtained for the combined TGA/DTA of CO₂ ads/des at 20°C for HX, A24, S4, and S2-25. These materials were selected as they covered the range of tether loadings observed, S2-25 having achieved the highest tether loading (1.8 tethers per nm²). These records show that each product gains mass very rapidly over the first few minutes under CO₂ flow. Then, in each case, the rate of adsorption becomes much slower, reaching an apparent equilibrium adsorption capacity after ~15 minutes. Each product subsequently desorbs most of this mass under the Ar purge, at first rapidly and then more slowly; however in each case desorption is incomplete. It can be seen that desorption from the aminopropyl-functionalized materials proceeds less readily than from the substrate and, furthermore, that the amount of adsorbed mass retained at the end of each desorption cycle is essentially inversely proportional to the N content of the materials. It should also be noted that this residual CO₂ was fully desorbed when the samples were subsequently heated to 150°C under Ar purge.

Table 2 lists the CO₂ adsorption capacities determined for these products at 20°C. These results show that the adsorption capacities of the sonication products are greater than that of the conventionally prepared product. The substrate has the least sorption capacity. Thus these results show that the sonication method does indeed lead to products with higher CO₂ capacities than the conventional synthesis method. The higher CO₂ capacities are attributed to the higher tether loadings, the contribution due to any residual template material being considered insignificant.

Table 2 lists $H_{\text{ads}}(\text{CO}_2)$ determined for these products at 20°C. These results show that $H_{\text{ads}}(\text{CO}_2)$ determined for the sonication products are each greater than that of the conventionally prepared product; $H_{\text{ads}}(\text{CO}_2)$ for the substrate is even lower as expected. Hence these results show that the sonication products overall bind CO₂ more strongly than the conventionally prepared product consistent with their higher tether loadings and so lead to reduced desorption at 20°C.

TABLE 2: Product CO₂ adsorption capacities, heats of adsorption of CO₂, and amine efficiencies.

	20°C			75°C		
	CO ₂ capacity (wt%)	$H_{\text{ads}}(\text{CO}_2)$ (kJ·mol ⁻¹)	CO ₂ per N (mol·mol ⁻¹)	CO ₂ capacity (wt%)	$H_{\text{ads}}(\text{CO}_2)$ (kJ·mol ⁻¹)	CO ₂ per N (mol·mol ⁻¹)
^a ±error	0.2	4	—	<0.1	6	—
HX	3.7	36	n/a	1.1	53	n/a
A24	4.4	47	0.60	1.6	61	0.22
S4	5.3	51	0.62	2.0	70	0.23
S2-25	4.9	60	0.54	1.9	90	0.21

^aError estimated from the average of standard deviation obtained for duplicate measurements taken for A24.

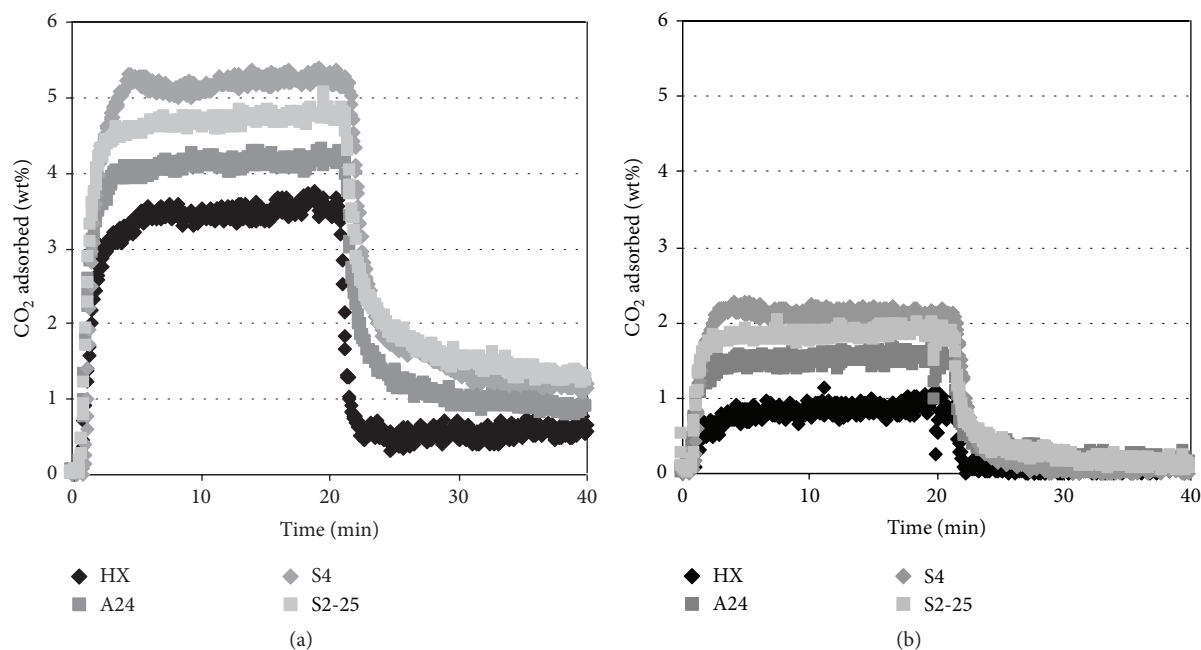


FIGURE 5: Typical mass flow records obtained for TGA of CO₂ sorption for selected materials (feed gas 90% CO₂/Ar (0–20 mins), 100% Ar (20–40 mins)) at (a) 20°C and (b) 75°C.

Table 2 also lists the amine efficiencies (the molar ratio of the amount of CO₂ adsorbed/N bound) calculated for the functionalized products studied. These results show that the sonication products each exhibited amine efficiencies greater than the theoretical limit for carbamate formation (0.5) consistent with some CO₂ adsorption occurring other than via ammonium carbamate formation (i.e., on residual silica type surface). Indeed it is thought that ammonium carbamate formation is not as significant as other modes of adsorption at this temperature as will be discussed below (refer to CO₂ Adsorption/Desorption at 75°C).

3.2.2. CO₂ Adsorption/Desorption at 75°C. Figure 5 also shows the typical gravimetric records obtained for the combined TGA/DTA of CO₂ adsorption/desorption at 75°C for HX, A24, S4, and S2-25. These records show that sorption for each product proceeds similarly to that observed at 20°C. It is also noted that desorption is essentially complete for all products within the 20 min Ar purge at 75°C; therefore CO₂ adsorption is completely reversible at this temperature.

Table 2 lists the CO₂ adsorption capacities determined for these products at 75°C. These results show that the amounts of CO₂ adsorbed at 75°C are in each case less than that adsorbed at 20°C consistent with the higher process temperature preventing CO₂ adsorption on the weaker sorption sites. These results also show that the adsorption capacities of the sonication products are greater than that of the conventionally prepared product consistent with their higher tether loadings; the substrate has even less CO₂ capacity. It is also noted that the amount of CO₂ adsorbed at 75°C is only marginally greater than the amount of CO₂ remaining adsorbed on the materials studied at 20°C following the initial 20 minute desorption cycle. Hence it is conjectured that CO₂ adsorbed at 75°C is primarily bound via carbamate formation and that carbamate formation is not readily reversed at room temperature. It is thus evident from Figure 5 that carbamate formation and reversal proceed more rapidly at 75°C than at 20°C as would be expected.

Table 2 lists $H_{\text{ads}}(\text{CO}_2)$ determined for these products at 75°C. These results show that all products exhibit greater

$H_{\text{ads}}(\text{CO}_2)$ at 75°C than at 20°C and that $H_{\text{ads}}(\text{CO}_2)$ determined for the sonication products is each greater than that of the conventionally prepared product; $H_{\text{ads}}(\text{CO}_2)$ for the substrate is even lower as expected. Hence these results show that CO_2 is bound more strongly to the sonication products than to the conventionally prepared product.

Table 2 also lists the amine efficiencies calculated for the functionalized products studied. These amine efficiencies are a lot lower than those observed at 20°C and a lot less than would be expected for ammonium carbamate formation at all amine sorption sites (i.e., amine efficiency = 0.5). Hence it is concluded that only a fraction of the amine groups can readily bind CO_2 via carbamate formation. Given that two amines groups are required to work cooperatively to bind CO_2 via carbamate formation (refer to (1)) as reported by Leal et al. [12], the low amine efficiency is thought to be due to many of the amine groups having insufficient proximity to each other to facilitate carbamate formation. That the sonication products had higher amine efficiencies than the conventional product is consistent with their higher tether loading (closer proximity of tethers). It is thought that CO_2 adsorbed at 20°C involves weaker physisorption of CO_2 at N sites stabilized via interaction with the silica surface and, possibly, to sorption on the silica type surface alone in addition to the more strongly bound ammonium carbamate species. Hence it is thought that the smaller residual amount of CO_2 adsorbed at 20°C after the 20 min Ar purge is more indicative of the amount of CO_2 adsorbed via ammonium carbamate formation.

4. Conclusions

Aminopropyl-functionalised HMS products prepared with sonication were found to have higher aminopropyl-tether loadings than analogous products prepared via the conventional continuously stirred reactor technique. Sonication provided aminopropyl-functionalized HMS products with up to 1.8 tethers per nm^2 . Products prepared by sonication were also found to have greater CO_2 sorption capacities.

Tether loadings increased with sonication time, and so it was proposed that longer times might lead to even higher loadings. Tether loadings were also found to be affected by dispersion concentration; tether loadings improved up to a point but the improvement was no longer apparent at higher concentrations. It was also found that rinsing the crude product prior to curing had no effect on the tether loading achieved. Furthermore it was found that curing under N_2 rather than under vacuum had no effect on the tether loading achieved. Given that tether loadings increased with sonication time it would seem likely that increasing sonication would also improve tether loadings somewhat further still, at least up to a point. Furthermore, the results suggest that the sonication process was useful to aid the removal of residual C (template) trapped within the HMS substrate and so would have made more surface silanols available for silylation and thereby leading to higher tether loading.

The aminopropyl-functionalised sorbents were found to adsorb up to 5.3 wt% CO_2 at 20°C; however the adsorption capacities were significantly smaller at 75°C (2.0 wt%). The

reduction in adsorption capacity was accompanied with an increase in $H_{\text{ads}}(\text{CO}_2)$ consistent with the reduced significance of weakly adsorbed CO_2 at the higher process temperature. These results suggest that many tethered N groups do not form ammonium carbamate species at 20°C; it is thought that such groups are likely to facilitate CO_2 adsorption via some other mechanism, such as weak physisorption at N sites stabilized via interaction with the silica surface and/or on residual nonfunctionalized regions of silica surface.

Conflict of Interests

The authors declare that there is no conflict of interests regarding the publication of this paper.

Acknowledgments

The authors thank Mr. Rod Mackie (Monash University School of Physics & Materials Engineering) for collecting the raw XRD data. The authors also thank the Australian Government for funding through their Australian Research Council and Cooperative Research Centre programs.

References

- [1] N. Stern and G. Treasury, *The Economics of Climate Change: The Stern Review*, Cambridge University Press, New York, NY, USA, 2007.
- [2] IPCC, *Climate Change 2007: Synthesis Report*, Intergovernmental Panel on Climate Change, 2007.
- [3] R. Garnaut, *The Garnaut Climate Change Review*, Cambridge University Press, Port Melbourne, Australia, 2008.
- [4] D. S. Kaufman, D. P. Schneider, N. P. McKay et al., "Recent warming reverses long-term arctic cooling," *Science*, vol. 325, no. 5945, pp. 1236–1239, 2009.
- [5] IEA, *CO₂ Emissions from Fuel Combustion (Highlights), Volume 2012*, International Energy Agency, 2012.
- [6] UNFCCC, *Kyoto Protocol to the United Nations Framework Convention on Climate Change*, UNFCCC, Bonn, Germany, 2007.
- [7] P. J. Cook, "Carbon dioxide capture and geological storage: research, development and application in Australia," *International Journal of Environmental Studies*, vol. 63, no. 6, pp. 731–749, 2006.
- [8] R. Davidson, *Post-Combustion Carbon Capture from Coal Fired Plants—Solvent Scrubbing*, IEA Clean Coal Centre Reports, 2007.
- [9] G. P. Knowles, J. V. Graham, S. W. Delaney, and A. L. Chaffee, "Aminopropyl-functionalized mesoporous silicas as CO_2 adsorbents," *Fuel Processing Technology*, vol. 86, no. 14–15, pp. 1435–1448, 2005.
- [10] A. Sayari, "Modified adsorbent for dry scrubbing of CO_2 and other acid gases," Patent WO2004054708A2, p. 41, University of Ottawa, Ottawa, Canada, 2004.
- [11] R. L. Burwell Jr. and O. Leal, "Modified silica gels as selective adsorbents for sulphur dioxide," *Journal of the Chemical Society, Chemical Communications*, no. 9, pp. 342–343, 1974.

- [12] O. Leal, C. Bolivar, G. Sepulveda, G. Molleja, G. Martinez, and L. Esparragoza, "Carbon dioxide adsorbent and method for producing the adsorbent," Patent US 5,087,597, Armada de la Republica de Venezuela, Universidad Central de Venezuela, Caracas, Venezuela, 1992.
- [13] A. Walcarius, M. Etienne, and J. Bessière, "Rate of access to the binding sites in organically modified silicates. I. Amorphous silica gels grafted with amine or thiol groups," *Chemistry of Materials*, vol. 14, no. 6, pp. 2757–2766, 2002.
- [14] A. L. Chaffee, "Molecular modeling of HMS hybrid materials for CO₂ adsorption," *Fuel Processing Technology*, vol. 86, no. 14-15, pp. 1473–1486, 2005.
- [15] M. V. Landau, L. Vradman, M. Herskowitz, Y. Koltypin, and A. Gedanken, "Ultrasonically controlled deposition-precipitation: Co-Mo HDS catalysts deposited on wide-pore MCM material," *Journal of Catalysis*, vol. 201, no. 1, pp. 22–36, 2001.
- [16] A. Gedanken, "Sonochemistry and its application to nanochemistry," *Current Science*, vol. 85, no. 12, pp. 1720–1722, 2003.
- [17] G. P. Knowles and A. L. Chaffee, *Aminopropyl-Functionalised Silica CO₂ Adsorbents via Sonochemical Methods*, Paper #SA365, School of Chemical and Environmental Engineering, University of Nottingham, Nottingham, UK, 2007.
- [18] A. C. C. Chang, S. S. C. Chuang, M. Gray, and Y. Soong, "In-situ infrared study of CO₂ adsorption on SBA-15 grafted with γ -(aminopropyl)triethoxysilane," *Energy & Fuels*, vol. 17, no. 2, pp. 468–473, 2003.
- [19] N. Hiyoshi, K. Yogo, and T. Yashima, "Adsorption of carbon dioxide on amine modified SBA-15 in the presence of water vapor," *Chemistry Letters*, vol. 33, no. 5, pp. 510–511, 2004.
- [20] N. Hiyoshi, K. Yogo, and T. Yashima, "Adsorption of carbon dioxide on aminosilane-modified mesoporous silica," *Journal of the Japan Petroleum Institute*, vol. 48, no. 1, pp. 29–36, 2005.
- [21] M. L. Gray, Y. Soong, K. J. Champagne et al., "Improved immobilized carbon dioxide capture sorbents," *Fuel Processing Technology*, vol. 86, no. 14-15, pp. 1449–1455, 2005.
- [22] R. A. Khatri, S. S. C. Chuang, Y. Soong, and M. Gray, "Thermal and chemical stability of regenerable solid amine sorbent for CO₂ capture," *Energy & Fuels*, vol. 20, no. 4, pp. 1514–1520, 2006.
- [23] V. Zeleňák, M. Badaničová, D. Halamová et al., "Amine-modified ordered mesoporous silica: effect of pore size on carbon dioxide capture," *Chemical Engineering Journal*, vol. 144, no. 2, pp. 336–342, 2008.
- [24] P. Bollini, N. A. Brunelli, S. A. Didas, and C. W. Jones, "Dynamics of CO₂ adsorption on amine adsorbents. I. Impact of heat effects," *Industrial & Engineering Chemistry Research*, vol. 51, no. 46, pp. 15145–15152, 2012.
- [25] A. Sayari and P. J. E. Harlick, "Functionalized adsorbent for removal of acid gases and its use," Patent WO2006094411A1, University of Ottawa, Ottawa, Canada, 2006.
- [26] A. Sayari and Y. Belmabkhout, "Stabilization of amine-containing CO₂ adsorbents: dramatic effect of water vapor," *Journal of the American Chemical Society*, vol. 132, no. 18, pp. 6312–6314, 2010.
- [27] P. Bollini, S. Choi, J. H. Drese, and C. W. Jones, "Oxidative degradation of aminosilica adsorbents relevant to postcombustion CO₂ capture," *Energy & Fuels*, vol. 25, no. 5, pp. 2416–2425, 2011.
- [28] M. Gil, I. Tiscornia, Ó. de la Iglesia, R. Mallada, and J. Santamaría, "Monoamine-grafted MCM-48: an efficient material for CO₂ removal at low partial pressures," *Chemical Engineering Journal*, vol. 175, no. 1, pp. 291–297, 2011.
- [29] G. P. Knowles, V. Beyton, and A. L. Chaffee, "New approaches for the preparation of aminopropyl-functionalized silicas as CO₂ adsorbents," *Preprints of Symposia—American Chemical Society, Division of Fuel Chemistry*, vol. 51, no. 1, pp. 102–103, 2006.
- [30] S. Ek, E. I. Iiskola, and L. Niinistö, "Gas-phase deposition of aminopropylalkoxysilanes on porous silica," *Langmuir*, vol. 19, no. 8, pp. 3461–3471, 2003.
- [31] S. Ek, E. I. Iiskola, L. Niinistö et al., "Atomic layer deposition of a high-density aminopropylsiloxane network on silica through sequential reactions of γ -aminopropyltrialkoxysilanes and water," *Langmuir*, vol. 19, no. 25, pp. 10601–10609, 2003.
- [32] A. Daehler, S. Boskovic, M. L. Gee, F. Separovic, G. W. Stevens, and A. J. O'Connor, "Postsynthesis vapor-phase functionalization of MCM-48 with hexamethyldisilazane and 3-aminopropyltrimethylethoxysilane for bioseparation applications," *The Journal of Physical Chemistry B*, vol. 109, no. 34, pp. 16263–16271, 2005.
- [33] G. P. Knowles, V. Beyton, and A. L. Chaffee, "CO₂ sorbents via aminoalkylsilane vapor treatment of hexagonal mesoporous silica," in *Proceedings of the International Symposium Nanoporous Materials—V (NANO '08): Program and Abstracts*, Vancouver, Canada, May 2008.
- [34] V. G. P. Sripathi, B. L. Mojet, A. Nijmeijer, and N. E. Benes, "Vapor phase versus liquid phase grafting of meso-porous alumina," *Microporous and Mesoporous Materials*, vol. 172, pp. 1–6, 2013.
- [35] S.-N. Kim, W.-J. Son, J.-S. Choi, and W.-S. Ahn, "CO₂ adsorption using amine-functionalized mesoporous silica prepared via anionic surfactant-mediated synthesis," *Microporous and Mesoporous Materials*, vol. 115, no. 3, pp. 497–503, 2008.
- [36] S. Hao, Q. Xiao, H. Yang, Y. Zhong, F. Pepe, and W. Zhu, "Synthesis and CO₂ adsorption property of amino-functionalized silica nanospheres with centrosymmetric radial mesopores," *Microporous and Mesoporous Materials*, vol. 132, no. 3, pp. 552–558, 2010.
- [37] W. Chaikittisilp, S. A. Didas, H.-J. Kim, and C. W. Jones, "Vapor-phase transport as a novel route to hyperbranched polyamine-oxide hybrid materials," *Chemistry of Materials*, vol. 25, no. 4, pp. 613–622, 2013.
- [38] G. P. Knowles, S. W. Delaney, and A. L. Chaffee, "Diethylenetriamine[propyl(silyl)]-functionalized (DT) mesoporous silicas as CO₂ adsorbents," *Industrial & Engineering Chemistry Research*, vol. 45, no. 8, pp. 2626–2633, 2006.
- [39] X. Xu, C. Song, J. M. Andresen, B. G. Miller, and A. W. Scaironi, "Novel polyethylenimine-modified mesoporous molecular sieve of MCM-41 type as high-capacity adsorbent for CO₂ capture," *Energy & Fuels*, vol. 16, no. 6, pp. 1463–1469, 2002.
- [40] G. P. Knowles, P. A. Webley, Z. Liang, and A. L. Chaffee, "Silica/polyethylenimine composite adsorbent S-PEI for CO₂ capture by vacuum swing adsorption (VSA)," in *Recent Advances in Post Combustion CO₂ Capture Chemistry*, M. Attala, Ed., vol. 1097, pp. 177–205, American Chemical Society, Washington, DC, USA, 2012.
- [41] W. Chaikittisilp, R. Khunsupat, T. T. Chen, and C. W. Jones, "Poly(allylamine)-mesoporous silica composite materials for CO₂ capture from simulated flue gas or ambient air," *Industrial*

- & *Engineering Chemistry Research*, vol. 50, no. 24, pp. 14203–14210, 2011.
- [42] P. T. Tanev and T. J. Pinnavaia, “A neutral templating route to Mesoporous molecular sieves,” *Science*, vol. 267, no. 5199, pp. 865–867, 1995.
- [43] M. W. McKittrick and C. W. Jones, “Toward single-site functional materials—preparation of amine-functionalized surfaces exhibiting site-isolated behavior,” *Chemistry of Materials*, vol. 15, no. 5, pp. 1132–1139, 2003.
- [44] K. C. Vranken, P. Van Der Voort, K. Possemiers, P. Grobet, and E. F. Vansant, “The physisorption and condensation of aminosilanes on silica gel,” in *Chemically Modified Surfaces*, J. J. Peseck and I. E. Leigh, Eds., pp. 46–57, Royal Chemistry Society, Cambridge, UK, 1994.

